Soft Matter

Dynamic Article Links

Cite this: *Soft Matter*, 2011, **7**, 2895

www.rsc.org/softmatter

PAPER

Transition between two orthogonal polar phases in symmetric bent-core liquid crystals

Lingfeng Guo,[a] Kinga Gomola,[a] Ewa Gorecka,[b] Damian Pociecha,[b] Surajit Dhara,[ac] Fumito Araoka,[a] Ken Ishikawa[a] and Hideo Takezoe*[a]

Received 30th October 2010, Accepted 14th December 2010
DOI: 10.1039/c0sm01233e

A unique phase transition between a uniaxial orthogonal phase with random polar order $\mathrm{SmAP_R}$ and orthogonal antiferroelectric phase $\mathrm{SmAP_A}$ is found in a series of symmetric achiral bent-core liquid crystals. The phase transition is weakly first order or continuous. The X-ray diffraction, electro-optical, optical second harmonic generation and dielectric methods, confirmed that the phase transition occurs from a locally polar ordered phase to a macroscopically antiferroelectrically ordered phase.

1. Introduction

Achiral liquid crystals made of bent-core molecules belong to a new class of materials for which the polar order is independent of molecular tilt. A number of new phases, that were not known for rod-like molecules, were discovered for these mesogens.[1–3] The bending of the molecular core causes a strong steric effect: the free rotation of molecules is hindered, leading to ordering of dipole moments. Either ferroelectric or antiferroelectric phases are possible depending on polar correlation between adjacent layers. However, it is rare for bent-core molecules to exhibit non-tilted phases. The compound showing both the conventional SmA phase and the polar "banana phase" $\mathrm{B_2}$ was first reported by Kovalenko *et al.*[4] and later on, a number of materials with non-polar uniaxial SmA phase were investigated.[5,6] Two other types of orthogonal non-polar smectic phase, composed of bent-core molecules, are the biaxial phase $\mathrm{SmA_b}$[7] and the $\mathrm{SmA_d}$ phase (interdigitated layer structure).[8] Nevertheless, the non-tilted biaxial smectic A phase with antiferroelectric behaviour, so-called the $\mathrm{SmAP_A}$ phase, was not experimentally proved until 2001 by Eremin *et al.*[9] In the following years, bent shaped compounds showing distinct polar orthogonal phases such as $\mathrm{SmA_dP_A}$ (interdigitated layer structure and antiferroelectric order),[10–12] $\mathrm{SmAP_R}$ (randomly distributed polar domains),[13,14] and $\mathrm{SmAP_{AR}}$ (randomly distributed antiferroelectric domains)[15] were synthesised and investigated.

The $\mathrm{SmAP_R}$ phase is interesting since it appears as uniaxial and non-polar, but the polar order can be easily induced by an external electric field. Because of the fast response under an electric field, the $\mathrm{SmAP_R}$ phase was confirmed to be a promising candidate for a new-generation fast switching liquid crystal display.[16] Although a few compounds showing a $\mathrm{SmAP_R}$ phase have been obtained,[17] the narrow temperature range of this phase is still a major limitation of utilizing this material in industry. Besides, not much is known about the polar order development in the orthogonal systems composed of bent-core molecules.

In this paper, we report a new phase sequence exhibited by a homologous series of bent shaped mesogens with 1,3-dihydroxyacetophenone as the central unit. These compounds are the first symmetric ones showing the $\mathrm{SmAP_R}$ phase.[18] Distinct from so far reported $\mathrm{SmAP_R}$ materials, which have a $\mathrm{B_{1RevTilted}}$ phase (a columnar phase made of layer fragments with 2D density modulation) as a lower temperature phase, this series of materials shows the antiferroelectric orthogonal phase ($\mathrm{SmAP_A}$) below the $\mathrm{SmAP_R}$ phase. Furthermore, the $\mathrm{SmAP_A}$ phase is maintained down to room temperature. It should be mentioned that recently Keith *et al.*[19] reported another series of compounds showing a similar phase sequence.

2. Experimental

The compounds were obtained according to the procedure reported in our previous paper.[18] Phase transition temperatures and associated enthalpy changes were determined by differential scanning calorimetry (DSC, Pyris Diamond Perkin-Elmer) and texture observation under a polarizing optical microscope (Nikon, Optiphot-pol) equipped with a heating stage (Mettler Toledo FP82). The DSC measurements were operated at a rate 10–20 °C $\mathrm{min^{-1}}$ on both heating and cooling runs. The X-ray diffraction patterns were recorded using Bruker D8 Discover and GADDS systems, for samples with homeotropic alignment, obtained by slow cooling of a drop of the isotropic liquid below the clearing temperature. The X-ray beam was directed almost parallel to the substrate surface.

The electro-optical and switching behaviours were obtained using a function generator (HP 3245A) connected with a high

---

[a] *Department of Organic and Polymeric Materials, Tokyo Institute of Technology, O-okayama, Meguro-ku, 152-8552, Tokyo, Japan. Fax: +81 3 5734 2876; Tel: +81 3 5734 2436*
[b] *Chemistry Department, Warsaw University, Al. Zwirki i Wigury 101, 02-089 Warsaw, Poland*
[c] *School of Physics, University of Hyderabad, 500046, India*

voltage amplifier (NF 4005). The polarization reversal current was measured across a 1 MΩ resistor using a standard triangular wave technique. In the birefringence measurement a Berek compensator (Nichika No.10547) was used. Dielectric measurements were done using a frequency response analyzer (Solartron 1255B) and dielectric interface (Solartron 1296) for planar cells. The glass substrates were coated with an indium-tin-oxide (ITO) electrode and polyimide (AL1254). The alignment layer was rubbed in antiparallel direction. The measuring field was 0.3 V_{pp}. The real and imaginary parts of dielectric permittivity from 0.1 Hz to 1 MHz were measured under different bias fields, up to 40 V. The dielectric strength $\Delta\varepsilon$ and relaxation frequency f_r were found by fitting measured data to the Cole–Cole formula.

In optical second-harmonic generation (SHG) measurements, a Nd:YAG laser (1064 nm, 8 ns duration, 10 Hz repetition) was used. The fundamental beam was cast upon the homogeneously aligned cells either at 45°. The SHG signal was detected in the transmission direction by a photomultiplier tube (R955, Hamamatsu) after blocking the fundamental light by an IR-cut filter. The signal was accumulated by a boxcar integrator (SR-250, Stanford Research System) for 30 s.

3. Results and discussion

The molecular structure, phase transition temperatures and related enthalpy changes for each compound are summarized in Table 1. Digits in the name of compound represent the number of carbon atoms in each terminal chain. ‘AP’ means 1,3-dihydroxyacetophenone as the central bent unit and ‘N’ stands for NO_2 group at both lateral positions. All of those compounds showed non-tilted smectic phases metastable down to room temperature. The temperature range of the $SmAP_R$ phase was broader than that of previously reported materials, reaching almost 50 °C for $n = 18$ and 20 compounds. The enthalpy change at the $SmAP_R$–$SmAP_A$ transition was small (~0.1 kJ mol^{-1}), indicating only weak structure difference between these two orthogonal phases.

In all studied materials, the layer spacing, *d*, shows noticeable negative thermal expansion in all temperature range of LC phases (Fig. 1(a)). Negative thermal expansion is typical for orthogonal smectic phases. It was observed in $SmAP_R$[17] and even in $SmAP_{AR}$[15] of other compounds. For compounds reported here, in the $SmAP_R$ phase *d* increases on cooling more apparently than in the $SmAP_A$ phase; the slope of *d vs. T* is ~0.2 Å K^{-1} for $SmAP_R$, which is an order of magnitude larger than observed for calamitic orthogonal smectics, and 0.03–0.05 Å K^{-1} for $SmAP_A$ with higher values for longer homologues. This implies that the mechanisms of layer spacing changes in each phase are different. The spacing in $SmAP_R$ phase is shorter than the molecular length *L*. The difference between *L* and *d* is in the order of magnitude of the length of the corresponding terminal aliphatic chain. Therefore, it is reasonable to assume that alkyl chains between adjacent layers are partially interdigited, as was also reported in the non-polar SmA phase composed of bent-core molecules.[4,6] In such non-polar phase, individual molecules rotate freely particularly at higher temperatures and the overall shape of rotating bent-core molecules can be regarded as bulky middle part with much thinner flexible molecular ends (Fig. 1(b) right). Packing of such objects into layers requires pronounced interdigitation of molecular tails between the layers to fill the space effectively. Of course, full interdigitation is not possible because of *gauche* conformations of flexible chains and their thermal dynamic motion. We expect that in the $SmAP_R$ phase with lowering temperature the rotation around the long molecular axis is frozen gradually as the coherence length for polar order is growing, resulting in a lower degree of interdigitation and thus an increase of layer thickness.

Table 1 Molecular structure of the studied compound and the phase transition temperatures (°C). Corresponding enthalpy changes (kJ mol^{-1}) of the transitions are listed in parentheses.

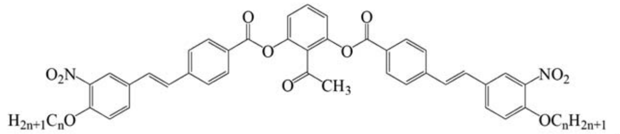

Code	n	$SmAP_A$		$SmAP_R$		Iso	ΔT $SmAP_R$
AP-14-NN-14	14	●	105.23 [0.03]	●	118.70 [5.70]	●	13.47
AP-16-NN-16	16	●	94.10 [0.20]	●	130.10 [4.73]	●	36.00
AP-18-NN-18	18	●	88.97 [0.18]	●	136.03 [3.67]	●	47.06
AP-20-NN-20	20	●	84[a]	●	134.70 [2.85]	●	50.70

[a] Determined by texture observation, since the corresponding DSC peak is too small.

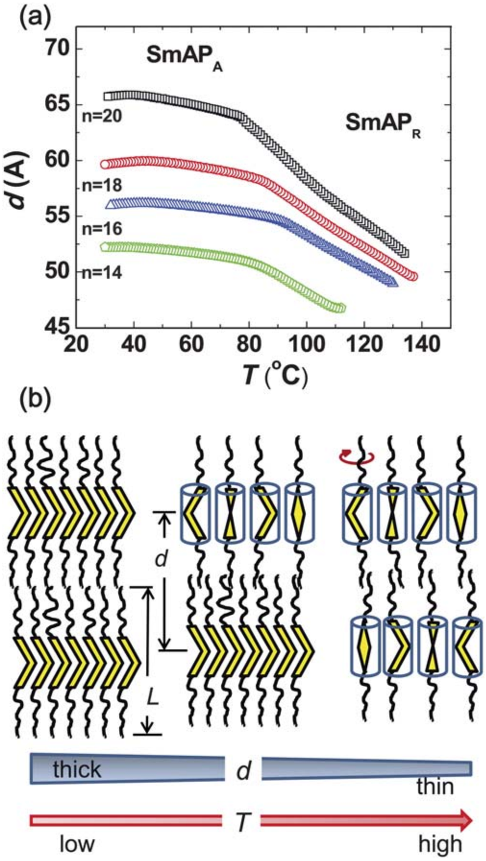

Fig. 1 (a) Layer spacing as a function of temperature measured on cooling, *n* denotes the length of the terminal alkyl chains. (b) Possible molecular packing in high, intermediate and low temperature ranges of the $SmAP_R$ phase. Because of the partially interdigitation of terminal chains, $d/L < 1$.

The situation is illustrated in Fig. 1(b). At higher temperatures, the size of the polar domains is very small, so that the molecules rotate almost freely, as mentioned above (Fig. 1(b) right). This is supported by SHG measurements (see Fig. 5 later); *i.e.*, SmAP$_R$ is SHG inactive under a certain field strength at higher temperatures. Since macroscopic polar order is induced *via* the Langevin process, *i.e.*, competition between polar interaction and thermal agitation, SHG does not emerge if the polar domain is too small to be oriented. The evolution of polar domains proceeds with decreasing temperature, since molecular packing becomes tight at lower temperatures. In the vicinity of the transition to the SmAP$_A$ phase, the adjacent layer correlation shown in Fig. 1(b) (left) is realized. For non-rotating molecules the efficient packing does not require strong interdigitation, since the cross section of the middle part of molecule is not much different than its end parts. In the intermediate temperature range, a situation shown in the middle of Fig. 1(b) may occur, since the evolution of the polar domain occurs dynamically. Thus the negative thermal expansion in SmAP$_R$ can be interpreted by the continuous variation of the ratio of the three typical situations shown in Fig. 1(b). In the SmAP$_A$ phase molecular rotation is frozen and layer spacing is larger than in the SmAP$_R$ phase, although it is still much smaller compared with the molecular length with fully extended chains. Moreover, the *d* value still increases with decreasing temperature. These facts suggest that the increase of layer spacing with decreasing temperature mainly originates from the increase of orientational order of long molecular axes and the change of the chain conformation (decreasing number of *gauche* conformations on cooling). These effects are also valid for the SmAP$_R$ phase.

If we compare the X-ray diffraction patterns of homeotropically aligned sample of AP-20-NN-20 in both phases (Fig. 2(a) and (b)) it is quite clear that although both have liquid like order inside the layer, the layers are much better defined for the SmAP$_A$ phase, as indicated by larger number of harmonics of the main signal. The diffuse character of wide-angle scattering, found even at ambient temperature, signifies a liquid-like disorder within layers. But it should be noticed that in the low temperature phase SmAP$_A$, the wide angle signal is slightly sharper than in the SmAP$_R$ phase, indicating larger correlation length of in-plane molecular ordering (Fig. 2(c)). The in-plane correlation lengths, obtained by fitting wide angle signal to Lorentz formula, in SmAP$_R$ and SmAP$_A$ are 2.4 Å and 4.8 Å, respectively.

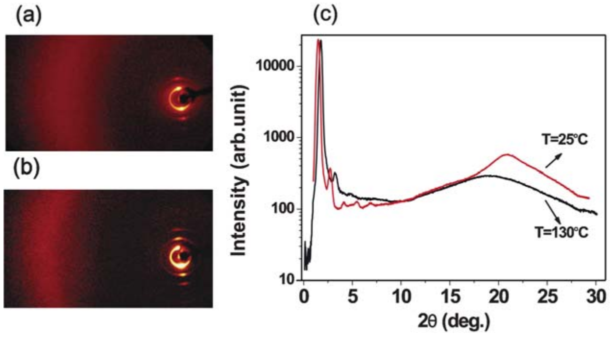

Fig. 2 Two dimensional X-ray patterns for compound AP-20-NN-20: (a) in the SmAP$_R$ phase at 130 °C, (b) in the SmAP$_A$ phase at 25 °C. Slight up/down asymmetry in the pattern is due to shadowing by sample heating stage. (c) Intensity *vs.* 2θ obtained by integration of 2D patterns over azimuthal angle at 130 °C and 25 °C, respectively.

Texture observation is always useful to identify the phase behaviour. In the homeotropic cells, aligned by polyimide SE1211, a uniform dark image was observed in the SmAP$_R$ phase indicating macroscopic uniaxiality. On cooling birefringent texture slowly appears indicating the transition from uniaxial (SmAP$_R$) to biaxial (SmAP$_A$) phase.[18] Fig. 3 shows focal conic textures of both phases, being characteristic to lamellar structures. By comparing Fig. 3(a) and (c), it can be clearly seen that the phase transition causes only a birefringence change in the texture. The extinction directions in both phases were parallel to the layer normal, certifying the orthogonal smectic phase. Under applying an electric field (20 V$_{pp}$/μm) (Fig. 3(b) and (d)) the birefringence slightly increases from 0.094 to 0.101 in the SmAP$_R$ and from 0.117 to 0.122 in the SmAP$_A$ phase. The higher value of the SmAP$_A$ compared to SmAP$_R$ in the field-on state, where all molecules are oriented with their dipole moments along the electric field, is caused by slightly higher orientational order of long molecular axes in the SmAP$_A$ phase. The reorientation of molecules under the field in both phases occurs without changing the optical extinction directions, which is also consistent with the orthogonal nature of the two phases.

Switching current was recorded on applying a triangular wave electric field to a planar cell at various temperatures. In the SmAP$_R$ phase, one broad peak for each half cycle was obtained as shown in Fig. 4(a). Such a peak can be attributed to the field-induced reorientation of local polar domains from random distribution to the field direction through a Langvin process, which is a typical behavior of the SmAP$_R$ phase.[14] In the lower temperature phase, SmAP$_A$, two current peaks per half cycle were detected (Fig. 4(b)), indicating that the ground-state structure of the mesophase is antiferroelectric. The spontaneous polarization (P_S) values calculated from the switching current in

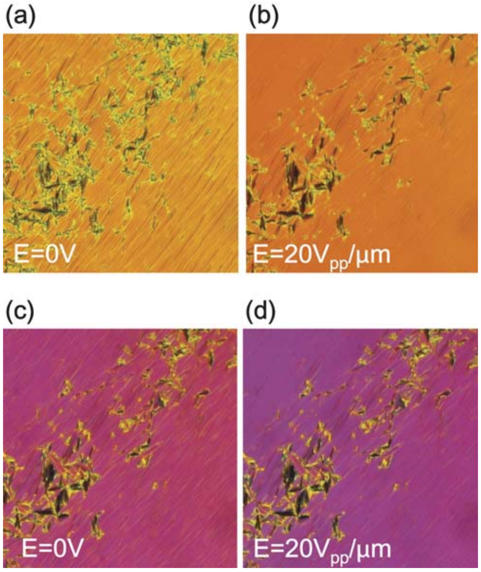

Fig. 3 Homogeneous textures of AP-18NN-18. (a) Field off state, $\Delta n = 0.094$, and (b) field-on state, $\Delta n = 0.101$ in the SmAP$_R$ phase at 103 °C. (c) Field off state, $\Delta n = 0.117$, and (d) field-on state $\Delta n = 0.122$, in the SmAP$_A$ phase at 85 °C. Cell thickness was 4.6 μm.

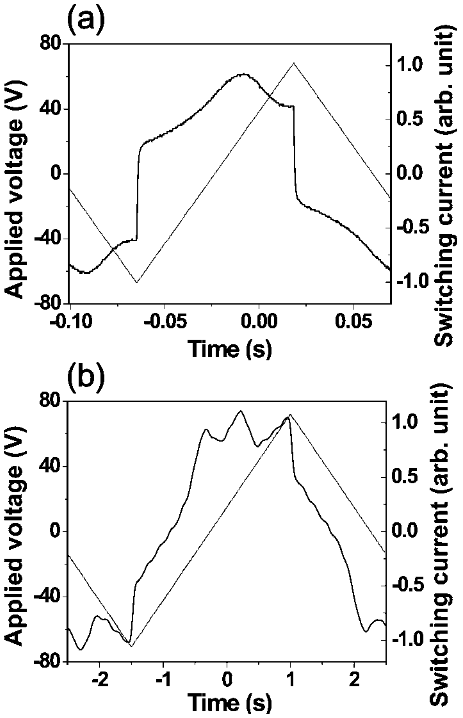

Fig. 4 Switching current response recorded by applying a triangular wave voltage to a 5.2 μm-thick cell. (a) SmAP$_R$ at 97 °C (140 V$_{pp}$, 6 Hz) and (b) SmAP$_A$ at 87 °C (140 V$_{pp}$, 0.2 Hz). In order to resolve the double switching current peak in SmAP$_A$ phase the frequency of the applied voltage has to be below 1 Hz.

SmAP$_R$ and SmAP$_A$ are ~170 nC cm^{-2} (97 °C) and ~300 nC cm^{-2} (87 °C), respectively.

The polar order in both phases was also monitored by the SHG method. The intensity of the SHG signal as a function of temperature with and without an applied electric field is given in Fig. 5. When the materials were tested without an electric field, no signal could be obtained at any temperature, indicating that neither of the two polar phases has macroscopic spontaneous polarization. Upon field application, polar order is easily induced in the SmAP$_R$ phase; *i.e.*, SH signal gradually increased on cooling and reached a maximum value near the SmAP$_R$ to SmAP$_A$ phase transition. That is because molecular dipoles cooperatively orient in the layer by the application of an electric field and with reducing temperature the coherence length gradually increases. On the contrary, in the low temperature phase, SmAP$_A$, the induction of polar order is associated with a threshold for the structure change from SmAP$_A$ to SmAP$_F$. Since this threshold voltage increases with lowering temperature, the SH signal under the same voltage decreases rapidly on cooling in SmAP$_A$ phase.

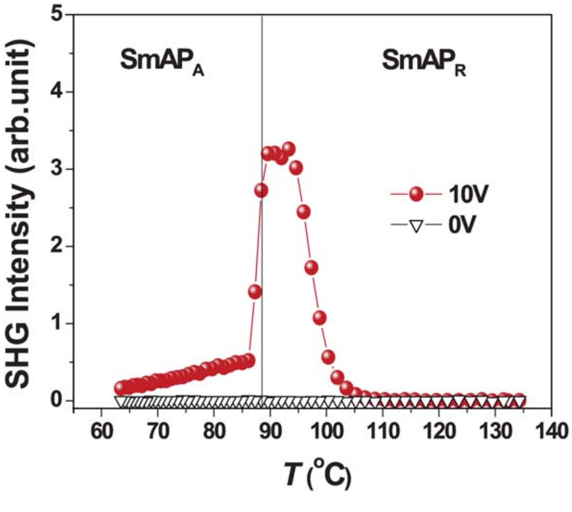

Fig. 5 Temperature dependence of the SHG intensity in a homogeneously aligned 4.8 μm-thick cell on cooling from the isotropic phase. Open triangles represent a zero field run and closed circles represent data obtained under applying dc 10 V to the sample.

The dielectric measurements were conducted in planar cells. The overall dielectric behaviour as functions of temperature and frequency is shown as a 3-D plot of imaginary part of dielectric permittivity (ε”) recorded in a cooling process (Fig. 6(a)). In the whole temperature range, two relaxation modes could be clearly seen. The higher frequency mode can be attributed to the non-collective motion of polar molecules, its relaxation frequency follows the Arrhenius law: $f_{Arrh} = f_0 e^{-E/kT}$ with activation energy E_a = 151 kJ mol^{-1}, and the dielectric strength slightly increases with reducing temperature. The lower frequency mode shows critical behaviour near the phase transition, thus can be attributed to collective movement of dipole moments. The relaxation

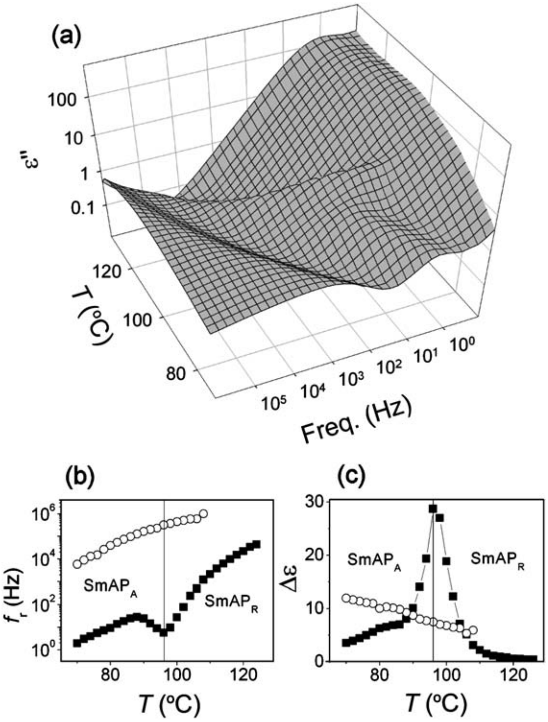

Fig. 6 (a) Three-dimensional (3D) plot of imaginary part of dielectric permittivity of AP-18NN-18 material. Two relaxation modes caused by cooperative motion and non-collective movement of dipole molecules can be seen at low and high frequencies, respectively. (b) Relaxation frequency f_r and (c) dielectric strength Δε of the both dielectric modes as a function of temperature. Homogeneous aligned cell with the thickness of 5.4 μm was used in the dielectric measurement.

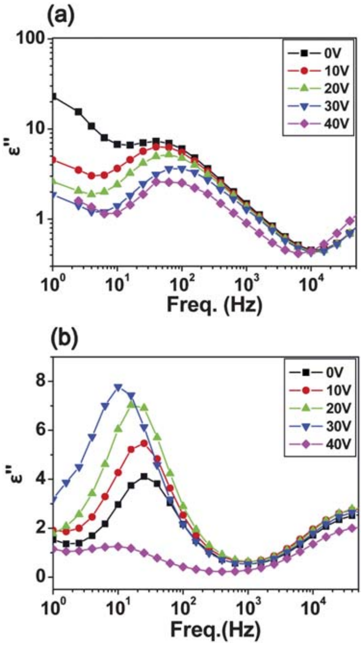

Fig. 7 Frequency dependence of imaginary part of dielectric permittivity in (a) $SmAP_R$ at 100 °C and (b) $SmAP_A$ at 80 °C under application of various dc bias fields.

frequency reaches the minimum (~3 Hz) and mode strength maximum (~30), at the phase transition, that indicates long living polar fluctuation in the system on approaching phase transition. Since f_r is proportional to the strength of interlayer polar interactions in the system (the stronger interaction the higher relaxation frequency)[20] its low value at T_c indicates that for studied material interlayer polar coupling is weak. The low dielectric response in the $SmAP_A$ phase is consistent with the proposed antiferroelectric model of this phase.

The effect of dc bias on the relaxation mode was also examined in both polar phases. In the $SmAP_R$ phase the relaxation frequency increased, simultaneously with decreasing dielectric strength, under increasing bias voltage (Fig. 7(a)). This is because bias filed suppresses the collective motion of molecular dipoles. This behaviour is consistent with the expected ferroelectric-like characteristic of the $SmAP_R$ phase. By contrast, in the $SmAP_A$ phase, dc bias field causes at first the increase of dielectric strength of the mode and its shift to the lower frequency, due to partial distortion of antiferroelectric order in adjacent layers leading to the induction of non compensated polarization.[20] However the increase of the bias voltage above the threshold (the electric field required to impose ferroelectric state) results in nearly total suppression of the mode (Fig. 7(b)). The relaxation originating from non-collective movement of molecular dipoles is scarcely affected by a dc bias field.

4. Conclusion

The unique system showing transition from the uniaxial orthogonal phase with local polar order ($SmAP_R$) to the antiferroelectric non-tilted smectic phase ($SmAP_A$) was studied. Within the resolution of the used techniques (X-ray diffraction, dielectric and electro-optic), it seems that the transition is continuous or weakly first order, which is allowed for phases of different symmetry ($D_{\infty v}$ and D_{2h} for $SmAP_R$ and $SmAP_A$, respectively). The correlation length of polar order increases in the $SmAP_R$ phase gradually as well as antiferroelectric interlayer correlations. The interlayer polar coupling is weak as indicated by a low value of relaxation frequency of a ferroelectric mode at the phase transition. We suggest that the ferroelectric-like response in the $SmAP_R$ phase, identified by a single wide peak, occurs by collective reorientation of molecules in the layers.

References

1 H. Takezoe and Y. Takanishi, *Jpn. J. Appl. Phys.*, 2006, **45**, 597.
2 J. Etxebarria and M. B. Ros, *J. Mater. Chem.*, 2008, **18**, 2919.
3 R. A. Reddy and C. Tschierske, *J. Mater. Chem.*, 2006, **16**, 907.
4 W. W. Kovalenko, S. Grande, S. Diele, G. Pelzl and I. Wirth, *Liq. Cryst.*, 2000, **27**, 683.
5 I. Wirth, S. Diele, A. Eremin, G. Pelzl, S. Grande, L. Kovalenko, N. Pancenko and W. Weissflog, *J. Mater. Chem.*, 2001, **11**, 1642.
6 A. Eremin, H. Nadasi, G. Pelzl, S. Diele, H. Kresse, W. Weissflog and S. Grande, *Phys. Chem. Chem. Phys.*, 2004, **6**, 1290.
7 K. J. K. Semmler, T. J. Dingemans and E. T. Samulski, *Liq. Cryst.*, 1998, **24**, 799.
8 R. Pratibha, N. V. Madhusudana and B. K. Sadashiva, *Mol. Cryst. Liq. Cryst.*, 2001, **365**, 1711.
9 A. Eremin, S. Diele, G. Pelzl, H. Nadasi, W. Weissflog, J. Salfetnikolva and H. Kresse, *Phys. Rev. E: Stat. Phys., Plasmas, Fluids, Relat. Interdiscip. Top.*, 2001, **64**, 051707.
10 B. K. Sadashiva, R. A. Reddy, R. Pratibha and N. V. Madhusudana, *J. Mater. Chem.*, 2002, **12**, 943.
11 R. A. Reddy and B. K. Sadashiva, *J. Mater. Chem.*, 2004, **14**, 310.
12 L. Guo, S. Dhara, B. K. Sadashiva, S. Radhika, R. Pratibha, Y. Shimbo, F. Araoka, K. Ishikawa and H. Takezoe, *Phys. Rev. E*, 2010, **81**, 011703.
13 D. Pociecha, M. Cepic, E. Gorecka and J. Mieczkowski, *Phy. Rev. Lett.*, 2003, **91**, 18.
14 Y. Shimbo, E. Gorecka, D. Pociecha, F. Araoka, M. Goto, Y. Takanishi, K. Ishikawa, J. Mieczkowski, K. Gomola and H. Takezoe, *Phys. Rev. Lett.*, 2006, **97**, 113901.
15 K. Gomola, L. Guo, D. Pociecha, F. Araoka, K. Ishikawa and H. Takezoe, *J. Mater. Chem.*, 2010, **20**, 7944.
16 Y. Shimbo, Y. Takanishi, K. Ishikawa, E. Gorecka, D. Pociecha, J. Mieczkowski, K. Gomola and H. Takezoe, *Jpn. J. Appl. Phys.*, 2006, **45**, L282.
17 K. Gomola, L. Guo, S. Dhara, Y. Shimbo, E. Gorecka, D. Pociecha, J. Mieczkowski and H. Takezoe, *J. Mater. Chem.*, 2009, **19**, 4240.
18 K. Gomola, L. Guo, E. Gorecka, D. Pociecha, J. Mieczkowski, K. Ishikawa and H. Takezoe, *Chem. Commun.*, 2009, 6592.
19 C. Keith, M. Prehm, Y. P. Panarin, J. K. Vij and C. Tschierske, *Chem. Commun.*, 2010, **46**, 3702.
20 D. Pociecha, E. Gorecka, M. Čepič, N. Vaupotič, K. Gomola and J. Mieczkowski, *Phys. Rev. E*, 2005, **72**, 060701.